European Food Research and Technology (2022) 248:2591–2602
https://doi.org/10.1007/s00217-022-04072-1

ORIGINAL PAPER

Development and evaluation of an automated solvent-assisted flavour evaporation (aSAFE)

Philipp Schlumpberger[1] · **Christine A. Stübner**[1] · **Martin Steinhaus**[1]

Received: 13 April 2022 / Revised: 14 June 2022 / Accepted: 18 June 2022 / Published online: 4 July 2022

Abstract

Artefact-avoiding isolation of the volatiles from foods is a crucial step before analysis of odour-active compounds by gas chromatography (GC). In the past 20 years, solvent extraction followed by solvent-assisted flavour evaporation (SAFE) has become the standard approach, particularly prior to GC–olfactometry. The manual valve of the SAFE equipment, however, leads to suboptimal yields and the risk of a contamination of the volatile isolate with non-volatiles. We thus developed an automated SAFE (aSAFE) approach by replacing the manual valve with an electronically controlled pneumatic valve. The aSAFE provides clearly higher yields than the manual SAFE (mSAFE), notably from extracts high in lipids and for odorants with comparably high boiling points. Additionally, aSAFE substantially reduces the risk of non-volatiles being transferred to the volatile isolate. Full automatisation is possible by combining the aSAFE approach with an automated liquid nitrogen refill system as well as an endpoint recognition and shut-off system.

Keywords Automated solvent-assisted flavour evaporation · aSAFE · Volatile isolation · Yield · Gas chromatography–olfactometry

Introduction

The isolation of the volatile fraction from foods and beverages is a big challenge, in particular for flavour chemists engaged in the analysis of odour-active compounds with gas chromatographic methods such as gas chromatography–olfactometry (GC–O) [1]. Steam distillation approaches [2] widely used in the early days of GC lead to thermal compound degradation and artefact formation associated with the elevated temperatures [3–6]. Direct injection of solvent extracts without further purification as well as solid phase extraction approaches such as solid phase microextraction (SPME) [7] and stir bar sorptive extraction (SBSE) [8] requires hot injection techniques that also foster thermal degradation and artefact forming reactions (examples in [1, 6, 9, 10]).

The first researchers who clearly addressed the problem of artefact formation in odorant analysis were Weurman et al. [11]. They suggested a new and mild approach for the isolation of food volatiles for which they coined the name "high vacuum transfer" (HVT). In an evacuated system, two round-bottom flasks were connected with a glass tube. Flask 1 contained the food sample and was kept at room temperature, whereas flask 2 was initially empty. When flask 2 was cooled to –180 °C, the food volatiles evaporated in flask 1 and recondensed in flask 2, driven by the different vapour pressures associated with the temperature difference between the flasks. In 1985, Schieberle and Grosch adopted the HVT approach to separate the volatiles and the non-volatiles of extracts obtained from foods with low-boiling solvents such as diethyl ether, dichloromethane, or pentane [12]. A round-bottom flask containing the extract was connected with a glass tube to a series of gas washing bottles serving as cold traps. First, the extract was cooled down with liquid nitrogen. Then, the device was evacuated and cooling was applied to the cold traps, while the cooling of the extract was stopped. As a result, a temperature difference between the frozen extract and the cold traps developed,

Philipp Schlumpberger and Christine A. Stübner have contributed equally to this study and share first authorship.

✉ Martin Steinhaus
martin.steinhaus@tum.de

[1] Leibniz Institute for Food Systems Biology at the Technical University of Munich (Leibniz-LSB@TUM), Lise-Meitner-Straße 34, 85354 Freising, Germany

causing the solvent and extracted volatiles to sublime and recondense in the cold traps. Evaporative cooling kept the temperature difference small, thus ensuring a smooth process until the transfer of the solvent was completed, which required ~ 1–2 h/100 mL. To reduce losses associated with a recondensation of volatiles before entering the cold traps, Sen et al. added a water-thermostated double-walled glass tube to connect the round bottom flask and the cold traps and applied temperatures of up to 50 °C [13]. Another HVT variant designed to increase volatile yields was introduced by Guth and Grosch [14]. Instead of placing the entire solvent extract in the round bottom flask before starting the transfer, the extract was introduced in numerous small portions by using a dropping funnel. Discontinuous extract delivery with a high flow over a short period of time was found crucial to properly transfer the extract from the funnel to the flask, maintain the high vacuum, and avoid blockage of the dropping funnel outlet by solidified fat from high-fat extracts. No cooling was applied to the flask; thus, each portion instantly vaporised in a spray-like manner. A major drawback of this "dynamic HVT" approach was the high risk of a transfer of non-volatiles in the form of small droplets. Therefore, in 1992 Jung et al. suggested to insert a splash protection adapter between the round bottom flask and the thermostated glass tube [15]. The adapter forced the vapour stream into hard direction changes; thus, droplets of non-volatiles were deposited at the walls of the adapter and did not reach the cold traps.

In 1999, Engel et al. [16] combined the major parts of the dynamic HVT equipment into a single glass device. For its application, they coined the name "solvent-assisted flavour evaporation" and the acronym SAFE. The equipment is illustrated in Fig. 1. The SAFE device included a dropping funnel with a manual needle valve stopcock used to introduce portions of the solvent extract into the evaporation flask, a double-walled water-thermostated middle part interconnecting the evaporation flask held at 30–40 °C with the recondensation flask held at–196 °C, and a safety cold trap protecting the vacuum pump in case of an operating error. The thermostatisation of the complete middle part significantly increased yields, particularly of volatiles with a high boiling point (b.p.), even though only moderate temperatures of 30–40 °C were applied to avoid the formation of thermal artefacts. Moreover, the tubing between the stopcock of the dropping funnel and the evaporation flask was included into the thermostated part, which prevented its blockage by the solidification of fats when extracts rich in lipids were applied to SAFE. Propeller-shaped glass barriers in the middle part effectively captured droplets of non-volatile material. Furthermore, the SAFE equipment required less bench space and was easier and faster to set up than the HVT equipment, allowing more samples to be processed per working day. Given all these advantages, it was not surprising that SAFE

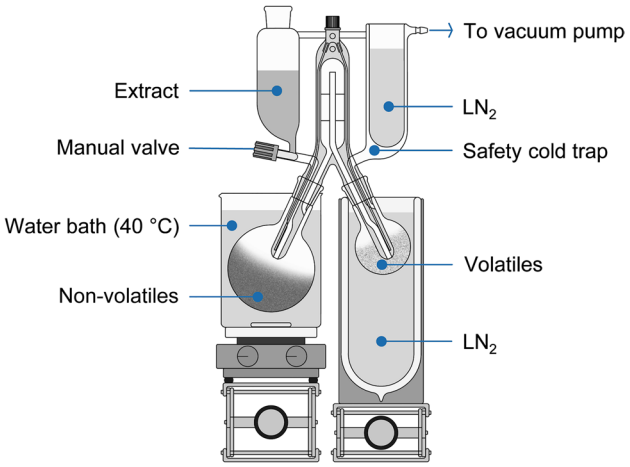

Fig. 1 Equipment for performing SAFE according to Engel et al. [16] (LN_2 = liquid nitrogen)

quickly became the standard approach for the artefact-avoiding isolation of volatiles in academic as well as in industrial food research. It has gained particular importance in the field of food odorants, where it is used to obtain representative volatile isolates suitable for GC–O screening. Between 1999 and 2022, the paper of Engel et al. received more than 600 citations [17].

Nevertheless, while successfully using SAFE for more than two decades in our laboratory, we yet identified some potential for improvement. One drawback of the SAFE approach is the high demand for manpower. During SAFE, the operator needs to be permanently present to open and close the manual valve of the dropping funnel. In addition, the liquid nitrogen level in the cold traps has to be monitored and the traps have to be refilled from time to time. A second drawback refers to yields. Engel et al. showed that SAFE yields of 100% can be achieved for volatiles with low boiling points, but yields decrease for compounds with higher boiling points and when lipids are present in the extract [16]. In addition, we suspected that yields may also differ between different operators and even between two experiments performed by the same operator. This might, for example, lead to problems when two SAFE volatile isolates are subjected to a parallel GC–O screening such as in a comparative aroma extract dilution analysis [1]. We assumed that the SAFE yields depend on the size of the individual extract portions introduced into the apparatus through the dropping funnel as well as on the time span between two portions. A reduction of the individual portion size in combination with an expansion of the time span between two portions was expected to lead to higher yields but would also increase the time required for completing the SAFE process. The third drawback is associated with the fact that large portion sizes might not only decrease the yield but beyond a certain limit they

lead to a significant transfer of non-volatiles to the volatile isolate, particularly when the extracts are rich in fat. In a brief moment of inattentiveness, even an experienced operator may once in a while fail to close the manual valve in appropriate time. Such an operating error eventually means that the volatile isolate is spoiled resulting in a waste of time, material, and manpower.

The drawbacks mentioned above are predominantly associated with the manual operation of the needle valve stopcock at the dropping funnel. The primary aim of the present study was therefore to replace the manual valve at the dropping funnel by an automated valve. The newly designed system was evaluated in terms of yields and finally further developed towards a fully automated SAFE system.

Materials and methods

Chemicals

Odorants **1**–**3**, **5**–**18**, and heptadecane were purchased from Merck (Darmstadt, Germany). Odorant **4** was from Thermo Fisher (Waltham, MA, USA). ($^2H_5$)-**13** and ($^2H_5$)-**16** were obtained from CDN Isotopes (Quebec, Canada). ($^2H_2$)-**9** was synthesised as described in the literature [18]. Dichloromethane (DCM) was purchased from CLN (Freising, Germany) and freshly distilled through a column (120 cm × 5 cm) packed with Raschig rings before use.

Food samples

A Bavarian style Pilsner beer, a dark chocolate (70% cocoa), and low odour sunflower oil, brand Thomy (Nestlé, Neuss, Germany) were purchased from a local supermarket.

SAFE equipment

All special glassware was custom-made by Glasbläserei Bahr (Manching, Germany). The pneumatic valve, type PT, the electronic valve control unit, type PAV 90, and the associated tubing were purchased from HWS Labortechnik (Mainz, Germany). The electronic valve control unit was supplied with compressed air at 300 kPa. The plunger of the pneumatic valve was exchanged for a custom-made polytetrafluoroethylene (PTFE) plunger by Glasbläserei Bahr. A PT 50 High Vacuum Pump System (Leybold, Cologne, Germany) ensured a vacuum of ≤ 0.01 Pa in the SAFE glassware. Major parts of the automated nitrogen refill system were purchased from KGW Isotherm (Karlsruhe, Germany). This included the siphon with the solenoid valve, the transfer hose, the nozzle with the phase separator, the Pt100 liquid nitrogen level sensors, the liquid nitrogen level control unit as well as the Dewar vessel for the recondensation flask and the safety cold trap. The latter was a 33 CAL shortened Dewar vessel with a diameter of 30 cm and a custom-made polyethylene top ring (Supplementary file 1, Fig. S1) with tension lock and holes for the sensors, the liquid nitrogen nozzle, a 500-mL recondensation flask (hole diameter 106 mm), and the safety cold trap (hole diameter 52 mm). The storage tank for the cryogenic liquefied nitrogen, type Apollo, volume 100 L, was purchased from Cryotherm (Kirchen/Sieg, Germany) and used pressurised at 70 kPa. The sensor used in the endpoint recognition and shut-off system was a type CFAM 12P1600 and purchased from Baumer (Frauenfeld, Switzerland). The sensor was secured by a 3D-printed polylactic acid (PLA) cap with hooks (Supplementary file 1, Table S1) attached to hooks on the glassware with a pair of elastomeric rings. The sensor was connected to an electronic endpoint control unit purchased from a local electrical engineer. The wiring diagram is available in the Supplementary file 1, Fig. S2.

Determination of SAFE yields with model mixtures

Individual stock solutions (10 mg/mL) were prepared from odorants **1**–**18** in DCM and checked for purity by GC–flame ionisation detector (FID) analysis of 1:100 dilutions. From the individual stock solutions and DCM, a working solution containing each odorant at a concentration of ~ 100 µg/mL was prepared and divided into 100 mL portions. Portions without further addition served as non-fat model mixture. Low-fat model mixtures and high-fat model mixtures were obtained by adding 1 g and 10 g of sunflower oil, respectively, to 100 mL portions of the working solution.

The model mixtures were subjected to different SAFE approaches. Individual model mixture/SAFE approach combinations were applied in triplicates. To each SAFE volatile isolate as well as to reference portions of the non-fat model mixture without SAFE treatment, 10 mL of a heptadecane solution (10 mg/mL) in DCM was added and the mixtures were analysed by GC–FID. Blank runs between sample injections were employed to demonstrate the absence of carry-over effects. For each GC run, peak areas corresponding to odorants **1**–**18** were divided by the peak area corresponding to the internal standard heptadecane to obtain the normalised peak areas. Normalised peak areas of three injections were averaged. Yields of the individual SAFE experiments were calculated by dividing the average of the normalised peak areas obtained after SAFE by the corresponding average of the normalised peak areas obtained without SAFE. Finally, the means and standard deviations were calculated from the yields obtained from the three experiments performed for each model mixture/SAFE approach combination as detailed in the Supplementary file 1, Tables S2–S12.

Determination of SAFE yields with beer and chocolate extracts

The beer was degassed by filtration through a folded filter. A portion of the filtrate (200 mL) was shaken with DCM (2 × 300 mL). Phase separation was achieved by centrifugation with a Heraeus Multifuge X3 FR (Thermo Fisher) at 10 °C and 4600 rpm for 20 min. The combined organic phases were washed with brine (2 × 100 mL) and dried over anhydrous sodium sulphate. The supernatant beer extract was used for the yield experiments.

The chocolate was cooled with liquid nitrogen, then coarsely crushed with a laboratory mill Grindomix GM 200 (Retsch, Haan, Germany), and finally ground into a fine powder with a 6875 Freezer Mill (SPEX SamplePrep, Stanmore, UK). The powder (250 g) was stirred with DCM (1000 mL) for 60 min. The mixture was dried over anhydrous sodium sulphate and centrifuged. The supernatant chocolate extract was used for the yield experiments.

Both, the beer and the chocolate extract were divided into ten aliquots, respectively, nine of which were used for further analysis. Three aliquots were used to determine the concentrations of odorants **9**, **13**, and **16** *before* SAFE. For this purpose, defined amounts of the stable isotopically substituted odorants ($^2H_2$)-**9**, ($^2H_5$)-**13**, and ($^2H_5$)-**16** in DCM solution were added as internal standards and the mixtures were subjected to SAFE. Aliquots 4–6 and 7–9 were used to determine the concentrations of odorants **9**, **13**, and **16** after application of different SAFE approaches. For this purpose, the stable isotopically substituted odorants were added to the volatile isolates *after* SAFE. The individual amounts added to the beer extract aliquots were 0.487 µg ($^2H_2$)-**9**, 152 µg ($^2H_5$)-**13**, and 5.19 µg ($^2H_5$)-**16**. The individual amounts added to the chocolate extract aliquots were 4.60 µg ($^2H_2$)-**9**, 27.1 µg ($^2H_5$)-**13**, and 51.9 µg ($^2H_5$)-**16**.

The concentrations of odorants **9**, **13**, and **16** in the beer and chocolate extracts before and after SAFE were finally determined by heart-cut GC–GC–mass spectrometry (GC–GC–MS) analysis of 1:5 dilutions of the volatile isolates (**13** in the beer extracts) or heart-cut GC–GC–MS analysis of concentrates (1 mL) obtained from the volatile isolates by using a Vigreux column (50 × 1 cm) and a Bemelmans microdistillation device [19] (**9** and **16** in the beer extract; **9**, **13**, and **16** in the chocolate extract). Odorant concentrations in the extract aliquots were calculated from the peak area counts of the analyte peak and the internal standard peak in the extracted ion chromatograms of characteristic quantifier ions, the aliquot volumes, and the amount of standard added, by applying a calibration line equation. The calibration line equation was obtained by linear regression after the analysis of analyte/standard mixtures in different concentration ratios. The analyte/standard ratios covered a range of ~ 5:1 to ~ 1:5.

The quantifier ions and the calibration line equations are summarised in the Supplementary file 1, Table S13. Concentration data is available in the Supplementary file 1, Tables S14–S19. Yields of the individual SAFE experiments were calculated by dividing the concentrations after SAFE by the concentrations before SAFE. Finally, the means and standard deviations were calculated from the yields obtained from the three experiments performed for each food extract/SAFE approach combination as detailed in the Supplementary file 1, Tables S20–S23.

GC–FID

A Trace 1310 Series gas chromatograph (Thermo Fisher) was equipped with a TriPlus RSH autosampler, a cold on-column injector, an FID, and a DB-FFAP column, 30 m length × 0.32 mm inner diameter (i.d.), 0.25 µm film thickness (Agilent, Waldbronn, Germany). The carrier gas was helium at 1.9 mL/min constant flow. The injection volume was 2 µL. The oven temperature was 40 °C for 2 min and then increased by 6 °C/min to 230 °C, which was held for 5 min. Data were acquired and evaluated by using the Chromeleon software, version 7.2.8 (Thermo Fisher).

Heart-cut GC–GC–MS

A Trace GC Ultra gas chromatograph (Thermo Fisher) was equipped with a Combi PAL autosampler (CTC Analytics, Zwingen, Switzerland), a cold on-column injector (Thermo Fisher), and a DB-FFAP column, 30 m length × 0.32 mm i.d., 0.25 µm film thickness (Agilent). The carrier gas was helium at a constant pressure of 100 kPa. The injection volume was 2 µL. The oven temperature was 40 °C for 2 min and then increased by 6 °C/min to 230 °C, which was held for 5 min. The end of the column was connected to a moving column stream switching (MCSS) system (Thermo Fisher) supplied with helium as make-up gas at 50 kPa. The MCSS system transferred the column effluent via deactivated fused silica capillaries (0.32 mm i.d.) time-programmed either simultaneously to an FID and a custom-made sniffing port [20] (230 °C base temperature) or via a heated (250 °C) hose to a liquid nitrogen-cooled trap inside the oven of a second gas chromatograph, which was a CP 3800 (Varian, Darmstadt, Germany) equipped with a DB-1701 column, 30 m length × 0.25 mm i.d., 0.25 µm film thickness (Agilent). The oven temperature was 40 °C for 2 min and then increased by 6 °C/min to 230 °C, which was held for 5 min. The end of the second column was connected to a Saturn 2200 ion trap mass spectrometer (Varian) operated in the chemical ionisation mode with methanol as the reagent gas and a scan range of *m/z* 60–250. Data were acquired and evaluated by using the MS Workstation software, version 6.42 (Varian).

Results and discussion

Design and application of the SAFE device with an automated valve

The device was largely based on the original SAFE device introduced by Engel et al. [16] (cf. Figure 1). The middle part including the connections to the thermostated evaporation flask and to the liquid nitrogen-cooled recondensation flask as well as the safety cold trap including the connection to the vacuum remained unchanged. The major modification was the exchange of the manual valve for a pneumatic valve. Minor modifications were required to the plunger casing and the dropping funnel. The new device is depicted in Fig. 2. Details on the modified parts are available in the Supplementary file 1, Fig. S3.

A pneumatic valve and the corresponding electronic control unit were purchased from a laboratory instruments supplier. To combine the pneumatic valve with the SAFE glassware, adjustments were necessary on both sides. The plunger supplied with the pneumatic valve was unsuitable to obtain sufficient tightness when the glassware was evacuated. It was therefore replaced by a custom-made PTFE plunger with a tapered tip. Tightness was achieved by an elastomeric O-ring. The O-ring was buried under the outer PTFE layer of the plunger to make sure that it was not a source of contamination. On the glassware side, a circumferential groove next to the orifice of the plunger casing accommodated a polymeric split washer as abutment for the union nut of the valve. If necessary, the position of the plunger was corrected with the adjustment screw of the pneumatic valve and the position of the adjustment screw was fixed with the set screw. The inner diameter of the glass tube connecting the body of the dropping funnel to the valve was reduced from ~ 7 to 1 mm. This modification was essential to achieve reasonably small extract portion sizes. With glass tube dimensions of 1 mm i.d. and 4 cm length, the flow through the open valve was ~ 3 mL/s when the glassware was under vacuum. The reduction in the size of this tube in combination with the weight of the pneumatic valve made it necessary to stabilise the glassware with an additional glass rod connecting the body of the dropping funnel and the plunger casing. The electronic valve control unit was supplied with compressed air. Depending on the switching state, PTFE tubes delivered the compressed air from the control unit to the pneumatic valve.

To perform a SAFE with the new device, it was mounted to a lattice lab system on the bench. The evaporation flask

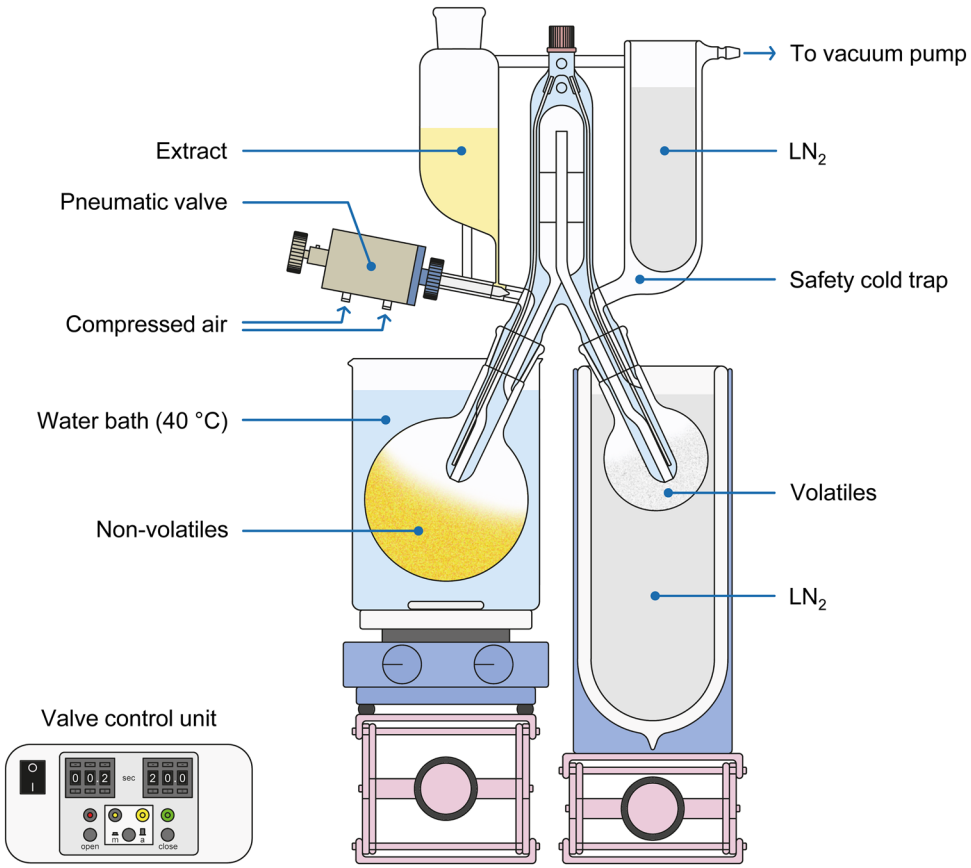

Fig. 2 Equipment for performing an automated SAFE including the pneumatic valve and its electronic control unit

and the recondensation flask were added and fixed with plastic joint clips. The middle part of the device was connected to the circulation thermostat and the water bath was applied to the evaporation flask. In both cases, the temperature was 40 °C. This value was found to be low enough to avoid thermal artefact formation and high enough to keep the lipid fraction of most food extracts in the liquid state.

The mode switch at the electronic valve control unit (Supplementary file 1, Fig. S4) was turned to manual and then the power supply was turned on at the main switch. With the open and close buttons, the correct operation of the valve was checked. With the valve in the closed position, the device was finally connected to the vacuum. After vacuum was established, the recondensation flask was cooled with liquid nitrogen. Then, the settings for the valve open time and the valve closed time were adjusted at the electronic control unit. Valve open times were set to 0.1–0.3 s equivalent to extract volumes of 0.3–0.9 mL. The valve closed times were set to 5–60 s. The selected valve closed time should at least be sufficient to allow for the complete evaporation of the solvent from the previous extract portion. Thus, the minimum setting depended on the valve open time as well as on the lipid content in the extract. High lipid contents clearly delayed the evaporation of the solvent.

As the next step, the extract was filled into the dropping funnel and the automated SAFE process was started by turning the mode switch to auto. Subsequently, the valve automatically switched between open and closed according to the settings. From time to time, liquid nitrogen needed to be added to the cold traps. When the extract level in the dropping funnel eventually reached the capillary at the bottom, the mode switch at the electronic valve control unit was turned to manual. This stopped the automated SAFE process. The cooling of the recondensation flask was removed, the device was ventilated, and the recondensation flask with the isolated volatiles was detached from the device.

The entire process of an automated SAFE is additionally described in a video provided on the internet [21]. To distinguish our new SAFE approach from the older SAFE approach with the manual valve, we suggest referring to the new approach as "automated SAFE" or "autoSAFE" and in writing use the abbreviation aSAFE. Whenever the original SAFE is addressed, we will from now on refer to it as manual SAFE or mSAFE.

Evaluation of the aSAFE approach

To determine the compound yields of the aSAFE approach in comparison to mSAFE, three different model mixtures, namely a non-fat model mixture, a low-fat model mixture, and a high-fat model mixture were prepared to simulate solvent extracts obtained from foods of different lipid content. The mixtures included 18 odorants in concentrations suitable for direct analysis by GC–FID. In their non-volatile lipid contents, the non-fat model mixture represented solvent extracts obtained from foods such as bread, fruit juice, or vegetables, the low-fat model mixture simulated solvent extracts from foods such as biscuits, milk, or meat products, and the high-fat model mixture resembled typical solvent extracts from foods such as chocolate, hard cheese, or nuts.

The 18 odorants used in the models were selected based on their occurrence and odour activity in food, their compound class, their boiling point, their log P value, their stability, and their GC retention behaviour (Table 1). In detail, all 18 compounds had been identified as important odour-active compounds in food [22]. For example, **1**, ethyl butanoate is a major odorant in different kinds of fruit such as strawberry, orange, guava, and kiwifruit [23–26] and **2**, 3-methylbutan-1-ol is a characteristic odorous fermentation by-product in bread [27, 28] as well as in alcoholic beverages such as beer, whisky, and wine [29–31]. The 18 compounds included hydrocarbons (**3**, **6**, **8**), alcohols (**2**, **4**, **9**, **13**), esters (**1**, **7**, **11**, **12**, **15**, **17**), carboxylic acids (**5**, **10**, **16**) as well as a ketone (**18**) and a phenol (**14**). Reactive compounds such as aldehydes and thiols were excluded to avoid interferences by degradation reactions. The 18 compounds covered a boiling point range of 120 to 271 °C, a log P value range of 1.10 to 4.82, and a retention index (RI) range of 1009 to 2555 on the FFAP column used for quantitation by GC–FID. Most importantly, all 18 compounds showed baseline separation during GC analysis.

The three model mixtures were subjected to mSAFE and aSAFE. To perform mSAFE, the operators were instructed to open the manual valve as short as possible to keep the portion sizes small. Before the next addition, complete evaporation and recondensation of the preceding portion was ensured visually. This was achieved by observing the evaporation flask and the liquid nitrogen surrounding the recondensation flask. During a recondensation phase, the liquid nitrogen showed vigorous boiling due to compensation of the heat of condensation, whereas complete recondensation was indicated by smoothening of the liquid nitrogen surface. For aSAFE, the valve open time was set to 0.2 s for all experiments. The valve closed time was varied and set to 5, 20, or 60 s. Of the resulting 12 different model mixture/SAFE approach combinations, however, the combination of the high-fat mixture and the aSAFE with 5 s valve closed time was not applicable, because 5 s was not sufficient to evaporate the solvent completely from the individual high-fat mixture portions.

As expected, the non-fat model mixture resulted in the highest yields (Fig. 3a). Compounds **1**–**13** with boiling points ranging from 120 to 220 °C showed yields of ~ 100% for both, the mSAFE (Fig. 3a, yellow bars) and the aSAFE (Fig. 3a, blue bars), and the reproducibility of the yields indicated by the error bars was good. Compounds **14**–**18**

Table 1 Food odorants in the model mixtures used for yield determinations

No.[a]	Odorant	Odour	b.p.[b] (°C)	Log P[c]	RI[d] FFAP
1	Ethyl butanoate	Fruity	120	2.85	1027
2	3-Methylbutan-1-ol	Malty	130	1.35	1206
3	α-Pinene	Resinous	156	4.44	1009
4	Hexan-1-ol	Grassy	157	2.03	1350
5	Butanoic acid	Cheesy, sweaty	162	1.10	1620
6	Myrcene	Geranium leaf	167	4.82	1156
7	Ethyl hexanoate	Fruity, pineapple	168	2.83	1226
8	Limonene	Citrusy, lime	177	4.38	1189
9	Linalool	Citrusy, bergamot	199	2.84	1539
10	Hexanoic acid	Cheesy, sweaty	203	1.75	1836
11	Ethyl octanoate	Fruity	207	4.47	1441
12	Ethyl benzoate	Fruity, star fruit	212	2.59	1658
13	2-Phenylethanol	Floral, honey	220	1.30	1905
14	Eugenol	Clove	254	1.83	2164
15	Methyl cinnamate	Sweet, cinnamon	261	2.62	2056
16	Phenylacetic acid	Beeswax	265	1.40	2555
17	Ethyl cinnamate	Sweet, fruity	271	2.90	2116
18	β-Ionone	Floral, violet	271	4.00	1933

[a]Numbering in the order of increasing boiling points

[b]Boiling point

[c]Common logarithm of the *n*-octanol–water partition coefficient

[d]Retention index

with boiling points of 254 °C and beyond, however, showed clear differences between the mSAFE and the aSAFE. mSAFE yields were consistently lower than aSAFE yields. We ascribed this effect primarily to the reduction of the individual extract portion volumes achieved by the aSAFE approach. Compounds **14**, eugenol and **15**, methyl cinnamate still showed aSAFE yields of ~ 100%, whereas mSAFE yields were ~ 80%. Compounds **17**, ethyl cinnamate and **18**, β-ionone showed aSAFE yields of > 90%, but mSAFE yields of only ~ 60%. Interestingly, the lowest yields were not determined for **18,** β-ionone, the compound with the highest boiling point, but for compound **16**, phenylacetic acid, thus suggesting that SAFE yields were not only influenced by the type of SAFE and the boiling points of the compounds, but also by the compound class.

The low-fat model mixture (Fig. 3b) in many cases showed lower yields than the non-fat model mixture (Fig. 3a). mSAFE yields of ~ 100% were obtained until compound **8**, limonene (b.p. 177 °C), with the exception of compound **5**, butanoic acid, for which the yield was ~ 90%. Beyond compound **8**, limonene, mSAFE yields decreased from ~ 80% (**9**, linalool) to ~ 6% (**18,** β-ionone). The decrease was not continuous. Instead, two compounds, namely **10**, hexanoic acid and **16**, phenylacetic acid, showed clearly lower yields. In summary, the yields of all three carboxylic acids (**9**, **10**, **16**) were lower than expected from their boiling points. This effect was also observed in all further experiments with mSAFE as well as with aSAFE. The aSAFE yields obtained from the low-fat model mixture were again consistently higher than the corresponding mSAFE yields. Moreover, aSAFE yields were higher when the valve closed times were longer. However, these differences were smaller than the differences between mSAFE and aSAFE. Thus, the reduction of the individual extract portion size obviously had a greater effect on the compound yields than the increase of the time span between two portions. For example, for compound **13**, 2-phenylethanol, the aSAFE approaches with 5, 20, and 60 s valve closed time showed yields of 92, 97, and 99%, but the yield of mSAFE was only 58%. The compound with the lowest yields was again compound **16**, phenylacetic acid. This compound showed aSAFE yields of 18, 22, and 44%, and an mSAFE yield of only 1%.

The high-fat model mixture (Fig. 3c) showed virtually the same mSAFE yields as the low-fat model mixture (Fig. 3b), but aSAFE yields were somewhat lower for compounds with high boiling points. Nevertheless, all aSAFE yields were still clearly higher than the corresponding mSAFE yields. Using again compounds **13**, 2-phenylethanol and **16**, phenylacetic acid as examples, the aSAFE approaches resulted in yields of 81–85% (**13**) and 6–10% (**16**), whereas mSAFE yields were only 58% (**13**) and 1% (**16**).

Different from the yields, no clear difference between mSAFE and aSAFE was found in the reproducibility. Error bars were generally small when yields were close to 100%

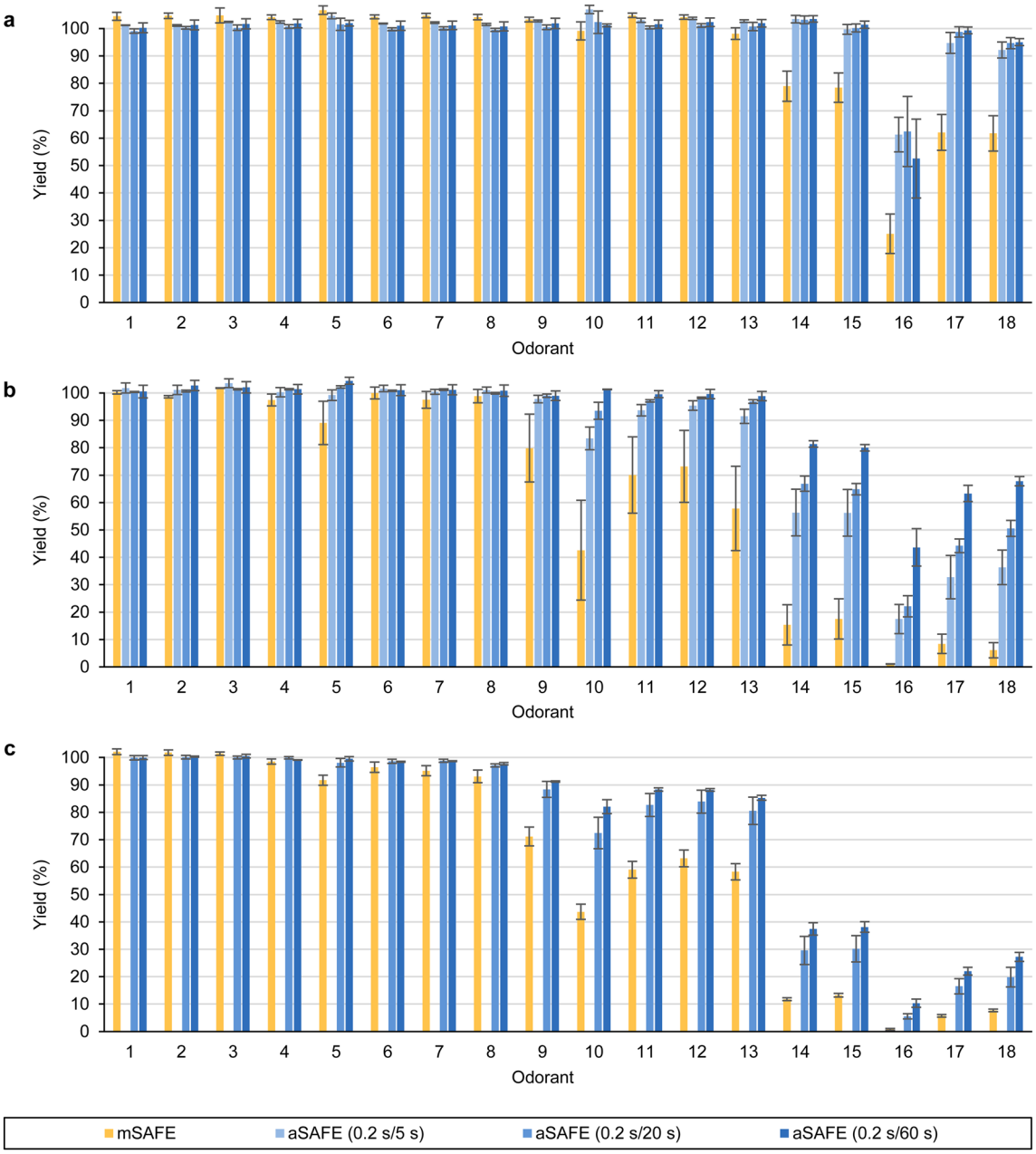

Fig. 3 Odorant yields of the aSAFE approach using valve open/closed time combinations of 0.2 s/5 s, 0.2 s/20 s, and 0.2 s/60 s in comparison to odorant yields of the mSAFE approach applied to three model mixtures of different fat content: **a**, non-fat; **b**, low-fat (100 mL non-fat mixture + 1 g oil); **c**, high-fat (100 mL non-fat mixture + 10 g oil). Odorant numbers refer to Table 1

and tended to increase in size when yields dropped, for both, mSAFE and aSAFE.

To evaluate the aSAFE approach further, we determined odorant yields from real food extracts. Beer and chocolate were chosen as a non-fat and a high-fat material, respectively. Odorants **9**, linalool; **13**, 2-phenylethanol; and **16**, phenylacetic acid were selected for quantitation, because they are present in both, beer [29] and chocolate [32]. The mSAFE approach was compared to aSAFE with a valve open/closed time combination of 0.2 s/60 s. Results are depicted in Figs. 4 and 5 in comparison to the yields obtained with the corresponding model mixtures.

The non-fat model mixture (Fig. 4a) and the beer extract (Fig. 4b) showed comparable yields. In both cases, yields of compounds **9**, linalool and **13**, 2-phenylethanol were close to 100%. The clearly higher absolute amount

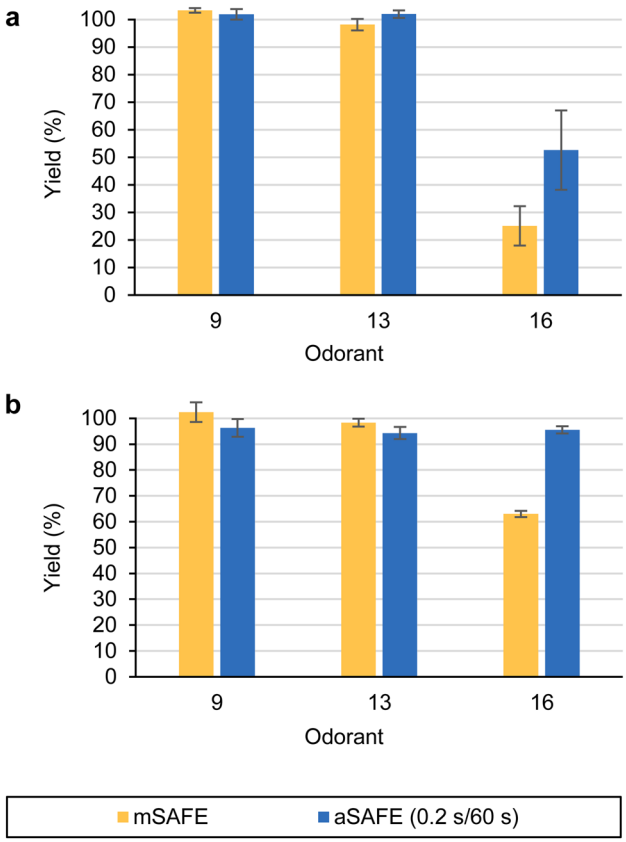

Fig. 4 Yields of compounds **9**, **13**, and **16** after application of the aSAFE approach with a valve open/closed time combination of 0.2 s/60 s, applied to the non-fat model mixture (**a**) and to the beer extract (**b**), in comparison to the yields of the mSAFE approach

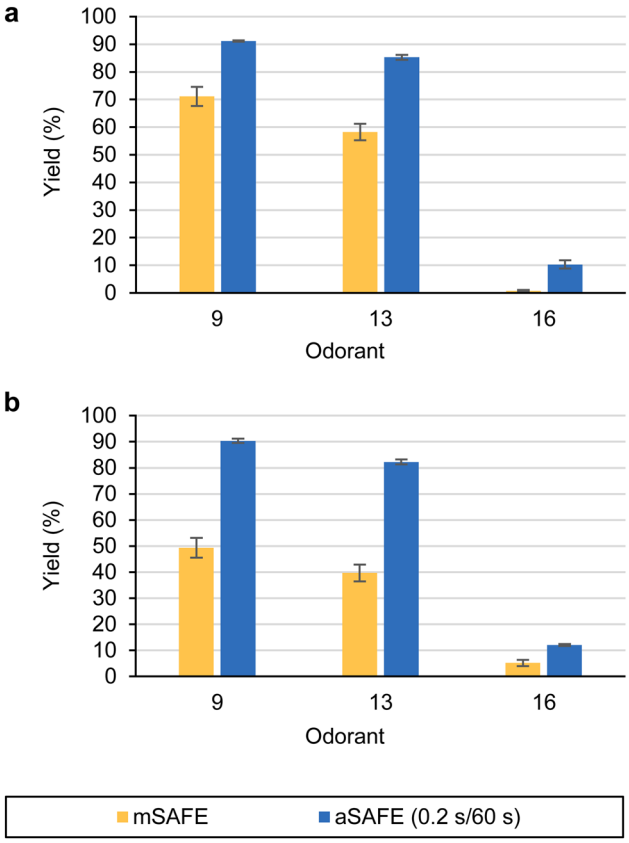

Fig. 5 Yields of compounds **9**, **13**, and **16** after application of the aSAFE approach with a valve open/closed time combination of 0.2 s/60 s, applied to the high-fat model mixture (**a**) and to the chocolate extract (**b**), in comparison to the yields of the mSAFE approach

of **13**, 2-phenylethanol in the beer extract, which was 8000 µg/L (Supplementary file 1, Table S14) compared to ~ 100 µg/L in the model mixture, obviously did not substantially influence the yield. The yields of **16**, phenylacetic acid were even higher from the beer extract than from the model mixture, however, again the aSAFE yield (96%) was clearly higher than the mSAFE yield (63%).

Likewise, the high-fat model mixture (Fig. 5a) and the chocolate extract (Fig. 5b) showed comparable yields. Again, the different absolute amounts of ~ 70 µg/L, ~ 400 µg/L, and ~ 1300 µg/L for compounds **9**, linalool; **13**, 2-phenylethanol; and **16**, phenylacetic acid in the chocolate extract (Supplementary file 1, Table S17) compared to ~ 100 µg/L for all three compounds in the model mixture, seemed to have only little influence on the yields. Particularly, the aSAFE yields were virtually the same. mSAFE yields were somewhat lower from the chocolate extract than from the model mixture for compounds **9**, linalool and **13**, 2-phenylethanol, but higher for compound **16**, phenylacetic acid. For all three compounds, yields from the chocolate extract were clearly higher when aSAFE was used instead of mSAFE.

Further automatisation of the aSAFE approach

With the aSAFE equipment depicted in Fig. 2, two of the major drawbacks of the mSAFE approach detailed in the introduction section were overcome: yields were clearly increased and "accidents" associated with too large extract portion sizes leading to a transfer of non-volatiles could be safely excluded. The manpower requirements, however, were only partly reduced. Although the operator does not need to manually open and close the valve of the dropping funnel anymore, there is still the need to refill the cold traps from time to time. Moreover, the operator is still required to be present towards the end of the aSAFE to stop the process at the electronic valve control unit as soon as there is only a minute amount of the extract left in the dropping funnel. Otherwise, uncontrolled ventilation of the apparatus could lead to damages to the vacuum system. Towards a fully automated SAFE, we therefore added an automated liquid nitrogen refill system as well as an endpoint recognition and shut-off system. The equipment is depicted in Fig. 6.

To supply both, the recondensation flask as well as the safety cold trap with the same automated liquid nitrogen

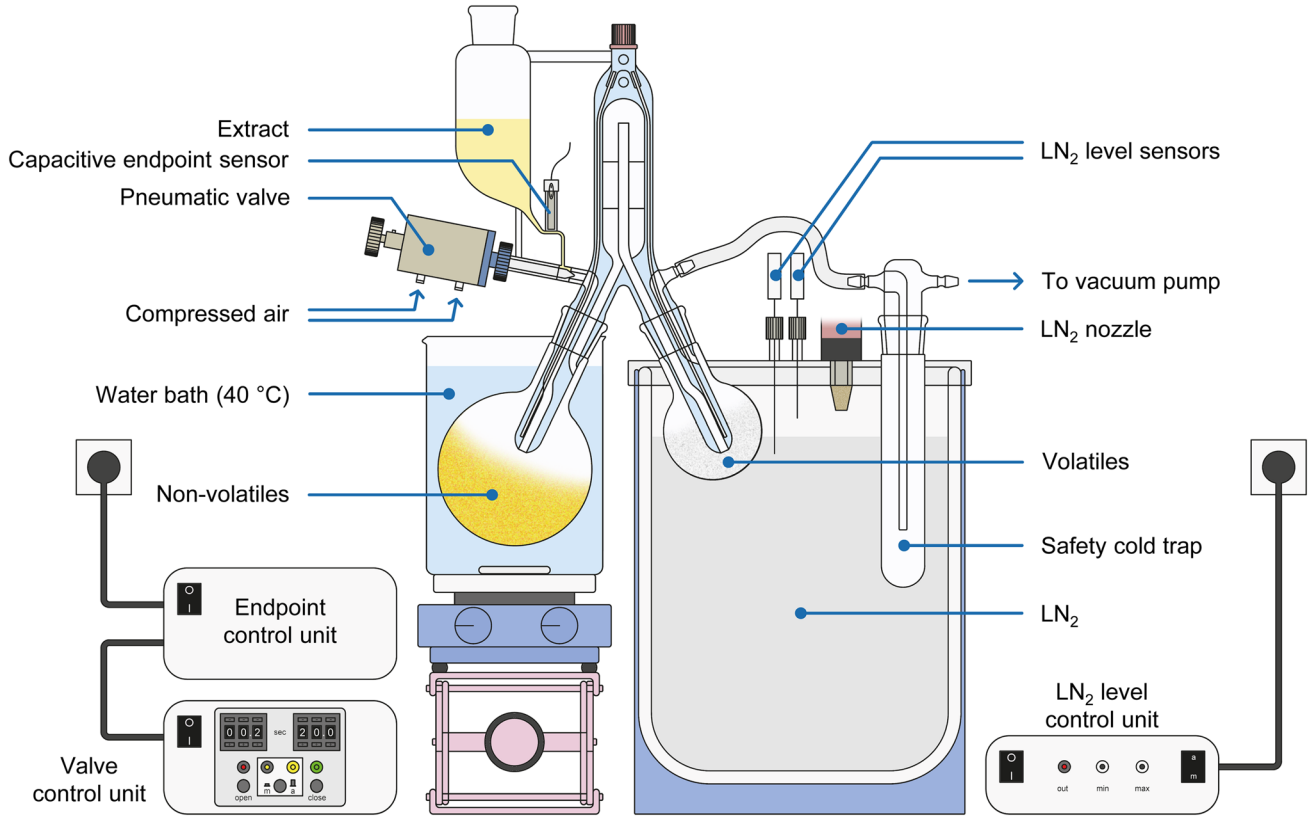

Fig. 6 Equipment for performing a fully automated SAFE including the pneumatic valve, the automated liquid nitrogen refill system as well as the endpoint recognition and shut-off system

refill system, the safety cold trap was separated from the SAFE glassware. The recondensation flask and the safety cold trap were placed in a Dewar vessel filled with liquid nitrogen. The automated nitrogen refill system consisted of a pressurised storage tank for cryogenic liquefied nitrogen with siphon, a solenoid valve, a transfer hose, a nozzle with phase separator, two liquid nitrogen level sensors, and an electronic liquid nitrogen level control unit operating the solenoid valve. The endpoint recognition and shut-off system consisted of a capacitive sensor and an electronic control unit. Adjustments were necessary in the glassware at the tube connecting the body of the dropping funnel with the valve. An additional glass cylinder served as casing for the sensor.

To perform a fully automated SAFE, the system is prepared and started as detailed for the aSAFE. Immediately thereafter, the liquid nitrogen level control unit is switched on. Whenever the liquid nitrogen level in the Dewar vessel drops below the level of the lower liquid nitrogen sensor, the liquid nitrogen level control unit opens the solenoid valve until the upper liquid nitrogen sensor is covered, thus ensuring sufficient cooling of the recondensation flask and the safety cold trap at all times. When finally the solvent extract level reaches the capacitive sensor at the outlet of the dropping funnel, the electronic endpoint control unit disconnects the electronic valve control unit operating the pneumatic valve from the power supply and thus stops the aSAFE process. The pneumatic valve remains closed, whereas the liquid nitrogen cooling is continued until the operator manually stops it before ventilating the system and collecting the isolated volatiles. A demonstration of a fully automated SAFE is available in a video provided on the internet [33].

Conclusion

The new aSAFE approach provides substantial advantages over mSAFE in terms of the yields of the volatiles and the risk of a transfer of non-volatiles. In our labs, aSAFE has meanwhile completely replaced the previous version. The fully automated SAFE equipment provides further advantages in the handling. However, the quality of the volatile isolate is not further improved when moving from the normal aSAFE to the fully automated equipment. Whether the improved handling of the fully automated equipment is worth the additional costs and workspace requirements is thus not a scientific but an economic question that may

be answered differently in an academic and an industrial environment, respectively.

Supplementary Information The online version contains supplementary material available at https://doi.org/10.1007/s00217-022-04072-1.

Acknowledgements We thank Julia Bock and Jörg Stein for excellent technical assistance, glassblower Wolfgang Bahr for brilliant ideas and continuous support, Budi Wöhrle for designing the electronic endpoint control unit, Daniel Kiehlmann for drawing the vector graphics, and Dr. Jürgen Behr for 3D printing. The videos provided as supplementary material on the internet were filmed and edited by the TUM ProLehre video production team. We thank Andreas Dunkel for the helpful advice on final video editing and video upload.

Funding Open Access funding enabled and organized by Projekt DEAL. The study was partially supported by funds of the Federal Ministry of Food and Agriculture (BMEL) based on a decision of the Parliament of the Federal Republic of Germany via the Federal Office for Agriculture and Food (BLE) under the innovation support programme (Grant No. 2816504314).

Declarations

Conflict of interest The authors declare that they have no conflict of interest.

Research involving human and animal studies This article does not contain any studies with human or animal subjects.

References

1. Steinhaus M (2019) Gas chromatography–olfactometry: principles, practical aspects and applications in food analysis. In: Tranchida P (ed) Advanced gas chromatography in food analysis. The Royal Society of Chemistry, Cambridge, pp 337–399
2. Chaintreau A (2001) Simultaneous distillation-extraction: from birth to maturity—review. Flavour Fragr J 16:136–148. https://doi.org/10.1002/ffj.967
3. Etievant PX (1996) Artifacts and contaminants in the analysis of food flavor. Crit Rev Food Sci Nutr 36:733–745. https://doi.org/10.1080/10408399609527746
4. Werkhoff P, Guntert M, Krammer G, Sommer H, Kaulen J (1998) Vacuum headspace method in aroma research: flavor chemistry of yellow passion fruits. J Agric Food Chem 46:1076–1093. https://doi.org/10.1021/jf970655s
5. Derail C, Hofmann T, Schieberle P (1999) Differences in key odorants of handmade juice of yellow-flesh peaches (*Prunus persica* L.) induced by the workup procedure. J Agric Food Chem 47:4742–4745. https://doi.org/10.1021/Jf990459g
6. Christlbauer M, Granvogl M, Schieberle P (2005) Development of a new stable isotope dilution assay for the quantitation of the intensely smelling onion odourant 3-mercapto-2-methylpentan-1-ol. In: Hofmann T, Rothe M, Schieberle P (ed) State-of-the-Art in Flavour Chemistry and Biology. Proceedings of the 7th Wartburg Symposium. Deutsche Forschungsanstalt für Lebensmittelchemie, Garching, Germany, pp 327–331
7. Lord H, Pawliszyn J (2000) Evolution of solid-phase microextraction technology. J Chromatogr A 885:153–193. https://doi.org/10.1016/s0021-9673(00)00535-5
8. Hasan CK, Ghiasvand A, Lewis TW, Nesterenko PN, Paull B (2020) Recent advances in stir-bar sorptive extraction: coatings, technical improvements, and applications. Anal Chim Acta 1139:222–240. https://doi.org/10.1016/j.aca.2020.08.021
9. Block E, Putman D, Zhao SH (1992) Allium chemistry: GC–MS analysis of thiosulfinates and related compounds from onion, leek, scallion, shallot, chive, and chinese chive. J Agric Food Chem 40:2431–2438. https://doi.org/10.1021/jf00024a018
10. Verhoeven H, Beuerle T, Schwab W (1997) Solid-phase microextraction: artefact formation and its avoidance. Chromatographia 46:63–66. https://doi.org/10.1007/bf02490931
11. Weurman C, Groenen PJ, van Gemert LJ (1970) Experiments on "high-vacuum transfer" in food odour research. Nahrung 14:607–616. https://doi.org/10.1002/food.19700140709
12. Schieberle P, Grosch W (1985) Photolyse von 13(S)-hydroperoxy-9(Z), 11(E)-octadecadiensäuremethylester in Gegenwart von Sauerstoff – Analyse der niedermolekularen Reaktionsprodukte. Fette Seifen Anstrichmittel 87:76–80. https://doi.org/10.1002/lipi.19850870209
13. Sen A, Laskawy G, Schieberle P, Grosch W (1991) Quantitative determination of beta-damascenone in foods using a stable isotope dilution assay. J Agric Food Chem 39:757–759. https://doi.org/10.1021/jf00004a028
14. Guth H, Grosch W (1989) 3-Methylnonane-2,4-dione – an intense odor compound formed during flavor reversion of soybean oil. Fett Wiss Technol 91:225–230. https://doi.org/10.1002/lipi.19890910604
15. Jung HP, Sen A, Grosch W (1992) Evaluation of potent odorants in parsley leaves [*Petroselinum crispum* (Mill.) Nym. ssp. *crispum*] by aroma extract dilution analysis. Lebensm Wiss Technol 25:55–60
16. Engel W, Bahr W, Schieberle P (1999) Solvent assisted flavour evaporation – a new and versatile technique for the careful and direct isolation of aroma compounds from complex food matrices. Eur Food Res Technol 209:237–241. https://doi.org/10.1007/s002170050486
17. Web of Science. Clarivate Analytics. https://apps.webofknowledge.com. Accessed 14 Jun 2022
18. Steinhaus M, Fritsch HT, Schieberle P (2003) Quantitation of (*R*)- and (*S*)-linalool in beer using solid phase microextraction (SPME) in combination with a stable isotope dilution assay (SIDA). J Agric Food Chem 51:7100–7105. https://doi.org/10.1021/jf0347057
19. Bemelmans JMH (1979) Review of isolation and concentration techniques. In: Land GG, Nursten HE (eds) Progress in flavour research. Applied Science, London, pp 79–98
20. Steinhaus M, Sinuco D, Polster J, Osorio C, Schieberle P (2008) Characterization of the aroma-active compounds in pink guava (*Psidium guajava*, L.) by application of the aroma extract dilution analysis. J Agric Food Chem 56:4120–4127. https://doi.org/10.1021/jf8005245

21. Schlumpberger P, Stübner CA, Steinhaus M (2022) Automated solvent-assisted flavour evaporation (aSAFE). Leibniz Institute for Food Systems Biology at the Technical University of Munich, Freising, Germany. https://youtu.be/_LnGns5As5s. Accessed 14 Jun 2022
22. Dunkel A, Steinhaus M, Kotthoff M, Nowak B, Krautwurst D, Schieberle P, Hofmann T (2014) Nature's chemical signatures in human olfaction: a foodborne perspective for future biotechnology. Angew Chem Int Ed 53:7124–7143. https://doi.org/10.1002/anie.201309508
23. Schieberle P, Hofmann T (1997) Evaluation of the character impact odorants in fresh strawberry juice by quantitative measurements and sensory studies on model mixtures. J Agric Food Chem 45:227–232. https://doi.org/10.1021/jf960366o
24. Buettner A, Schieberle P (2001) Evaluation of aroma differences between hand-squeezed juices from calencia late and navel oranges by quantitation of key odorants and flavor reconstitution experiments. J Agric Food Chem 49:2387–2394. https://doi.org/10.1021/jf001363l
25. Steinhaus M, Sinuco D, Polster J, Osorio C, Schieberle P (2009) Characterization of the key aroma compounds in pink guava (*Psidium guajava* L.) by means of aroma re-engineering experiments and omission tests. J Agric Food Chem 57:2882–2888. https://doi.org/10.1021/jf803728n
26. Lindhorst AC, Steinhaus M (2016) Aroma-active compounds in the fruit of the hardy kiwi (*Actinidia arguta*) cultivars Ananasnaya, Bojnice, and Dumbarton Oaks: differences to common kiwifruit (*Actinidia deliciosa* 'Hayward'). Eur Food Res Technol 242:967–975. https://doi.org/10.1007/s00217-015-2603-y
27. Schieberle P, Grosch W (1991) Potent odorants of the wheat bread crumb differences to the crust and effect of a longer dough fermentation. Z Lebensm-Unters Forsch 192:130–135. https://doi.org/10.1007/BF01202626
28. Rögner NS, Mall V, Steinhaus M (2021) Impact of malt extract addition on odorants in wheat bread crust and crumb. J Agric Food Chem 69:13586–13595. https://doi.org/10.1021/acs.jafc.1c05638
29. Fritsch HT, Schieberle P (2005) Identification based on quantitative measurements and aroma recombination of the character impact odorants in a Bavarian Pilsner-type beer. J Agric Food Chem 53:7544–7551. https://doi.org/10.1021/jf051167k
30. Poisson L, Schieberle P (2008) Characterization of the key aroma compounds in an American bourbon whisky by quantitative measurements, aroma recombination, and omission studies. J Agric Food Chem 56:5820–5826. https://doi.org/10.1021/jf800383v
31. Frank S, Wollmann N, Schieberle P, Hofmann T (2011) Reconstitution of the flavor signature of Dornfelder red wine on the basis of the natural concentrations of its key aroma and taste compounds. J Agric Food Chem 59:8866–8874. https://doi.org/10.1021/jf202169h
32. Chetschik I, Pedan V, Chatelain K, Kneubühl M, Hühn T (2019) Characterization of the flavor properties of dark chocolates produced by a novel technological approach and comparison with traditionally produced dark chocolates. J Agric Food Chem 67:3991–4001. https://doi.org/10.1021/acs.jafc.8b06800
33. Schlumpberger P, Stübner CA, Steinhaus M (2022) Fully automated solvent-assisted flavour evaporation. Leibniz Institute for Food Systems Biology at the Technical University of Munich, Freising, Germany. https://youtu.be/awd1NQsgbhY. Accessed 14 Jun 2022